Teresa Guarda
Filipe Portela
Manuel Filipe Santos (Eds.)

Communications in Computer and Information Science 1485

Advanced Research in Technologies, Information, Innovation and Sustainability

First International Conference, ARTIIS 2021
La Libertad, Ecuador, November 25–27, 2021
Proceedings

Springer

ARTIIS

Teresa Guarda · Filipe Portela ·
Manuel Filipe Santos (Eds.)

Advanced Research in Technologies, Information, Innovation and Sustainability

First International Conference, ARTIIS 2021
La Libertad, Ecuador, November 25–27, 2021
Proceedings

Springer

Editors
Teresa Guarda
Universidad Estatal Península de Santa Elena
La Libertad, Ecuador

Filipe Portela
Universidade do Minho
Guimarães, Portugal

Manuel Filipe Santos
Universidade do Minho
Guimarães, Portugal

ISSN 1865-0929 ISSN 1865-0937 (electronic)
Communications in Computer and Information Science
ISBN 978-3-030-90240-7 ISBN 978-3-030-90241-4 (eBook)
https://doi.org/10.1007/978-3-030-90241-4

This Springer imprint is published by the registered company Springer Nature Switzerland AG
The registered company address is: Gewerbestrasse 11, 6330 Cham, Switzerland

Preface

New digital evolution and transformation trends are enabling communication and ubiquitous computing between global citizens, industry, organizations, networked machines, and physical objects, providing a promising vision of the future integrating the real world of knowledge agents and things with the virtual world of information.

The current reality and the future of computing and communications are supported by a dynamic technological evolution in many fields, from wireless sensors and networks to nanotechnology.

Due to its broad impact in many fields, it has rapidly gained global attention from academia, governments, industry, and the general public. This change in the network of agencies profoundly modifies the landscape of human activity, particularly as regards knowledge acquisition and production, offering new possibilities but also challenges that need to be explored and assessed.

This book contains a selection of papers accepted for presentation and discussion at the International Conference on Advanced Research in Technologies, Information, Innovation, and Sustainability (ARTIIS 2021).

ARTIIS is an international forum for researchers and practitioners to present and discuss the most recent innovations, trends, results, experiences, and concerns from the perspectives of technologies, information, innovation, and sustainability.

The first edition of ARTIIS was realized this year, and it was a success. We received 155 contributions from authors in 37 countries around the world. The acceptance rate was 35.48%, with 53 regular papers and 2 short papers selected for presentation at the conference.

This conference had the support of the CIST Research and Innovation Center of Universidad Estatal Peninsula de Santa Elena, Ecuador, and the Algoritmi Research Center of the University of Minho, Portugal. It was realized in a hybrid format, taking place both taking place both online and in person at the Santa Elena Peninsula, Salinas, Ecuador, during November 25–27, 2021.

The Program Committee was composed of a multidisciplinary group of more than 122 experts from 25 countries, with the responsibility of evaluating, in a ‘double-blind review’ process, the chapters received for each of the main themes proposed for the conference: Computing Solutions, Data Intelligence, Ethics, Security, and Privacy and Sustainability.

- Computing Solutions addresses the development of applications and platforms involving computing for some area of knowledge or society. It includes topics like networks, pervasive computing, gamification, and software engineering.
- Data Intelligence focuses on data (e.g., text, images) acquisition and processing using smart techniques or tools. It includes topics like computing intelligence, artificial intelligence, data science, and computer vision.

- Ethics, Security, and Privacy considers a more strict and secure area of information systems where the end-user is the main concern. Vulnerabilities, data privacy, and cybersecurity are the main subjects of this topic.
- Sustainability explores a new type of computing which is more green, connected, efficient, and sustainable. Topics like immersive technology, smart cities, and sustainable infrastructure are part of this chapter.

The papers accepted are published in this volume in the Communications in Computer and Information Science series (CCIS), which is indexed in DBLP, Google Scholar, EI-Compendex, SCImago, and Scopus. CCIS volumes are also submitted for inclusion in ISI Proceedings.

ARTIIS 2021 included several special sessions held in parallel with the conference. These special sessions were as follows: ACMaSDA 2021 – Applications of Computational Mathematics to Simulation and Data Analysis; CICITE 2021 – Challenges and the Impact of Communication and Information Technologies on Education; ISHMC 2021 – Intelligent Systems for Health and Medical Care; IWEBTM 2021 – International Workshop on Economics, Business, and Technology Management; IWET 2021 – International Workshop on Electronic and Telecommunications; TechDiComM 2021 – Technological Strategies on Digital Communication and Marketing; and RTNT 2021 – Boost Tourism using New Technologies.

We acknowledge all of those who contributed to this book: authors, organizing chairs, the steering committee, the Program Committee, special sessions chairs, and editors. We deeply appreciate their involvement and support, which were crucial for the success of the International Conference on Advanced Research in Technologies, Information, Innovation, and Sustainability (ARTIIS 2021).

The success of this first edition gives us a lot of confidence to continue the work. So, we hope to see you in the second edition in 2022.

November 2021

Teresa Guarda
Filipe Portela
Manuel Filipe Santos

Organization

Honorary Chair

Brij Bhooshan Gupta	NIT Kurukshetra, India

General Chairs

Teresa Guarda	Universidad Estatal Peninsula de Santa Elena, Ecuador
Filipe Portela	University of Minho, Portugal

Program Committee Chairs

Teresa Guarda	Universidad Estatal Peninsula de Santa Elena, Ecuador
Filipe Portela	University of Minho, Portugal
Manuel Filipe Santos	University of Minho, Portugal

Organizing Chairs

Maria Fernanda Augusto	Universidad Estatal Peninsula de Santa Elena, Ecuador
Marcelo Leon	Universidad Tecnológica Empresarial de Guayaquil, Ecuador
Jose Maria Diaz-Nafria	Universidad a Distancia de Madrid, Spain
Isabel Lopes	Instituto Politécnico de Bragança, Portugal
Domingos Martinho	ISLA Santarem, Portugal
Sajid Anwar	Institute of Management Sciences, Pakistan

Steering Committee

Wolfgang Hofkirchner	Technische Universität Wien, Austria
Valentina Lenarduzz	LUT University, Finland
Bruno Sousa	University of Coimbra, Portugal
Ricardo Vardasca	ISLA Santarem, Portugal

Workshops Committee

Sajid Anwar	Institute of Management Sciences, Pakistan
Jose Maria Diaz-Nafria	Universidad a Distancia de Madrid, Spain
Teresa Guarda	Universidad Estatal Peninsula de Santa Elena, Ecuador

Program Committee

Abreu, Maria José	Universidade do Minho, Portugal
Alanis Garza, Arnulfo	Instituto Tecnologico de Tijuana, Mexico
Alcaraz, Cristina	Universidad de Malaga, Spain
Aljuboori, Abbas	University of Information Technology and Communications, Iraq
Almeida, Sofia	Universidade Europeia, Portugal
Alvarez, Francisco	Universidad Autónoma de Aguascalientes, Mexico
Alves, Victor	University of Minho, Portugal
Andrade, António	Universidade Católica Portuguesa, Portugal
Anselma, Luca	Università di Torino, Italy
Anwar, Sajid	Institute of Management Sciences, Pakistan
Arcos, Claudio	Fundación San Francisco Global, Ecuador
Augusto, Maria Fernanda	Universidad Estatal Peninsula de Santa Elena, Ecuador
Azevedo, Ana	Instituto Politécnico do Porto, Portugal
Bacca Acosta, Jorge Luis	University of Girona, Spain
Balaji G, Naveen	University of KwaZulu-Natal, South Africa
Balsa, Carlos	Instituto Politécnico de Bragança, Portugal
Bandurova, Inna	Oxford Brookes University, UK
Baras, Karolina	Universidade da Madeira, Portugal
Belli, Simone	Universidad Complutense de Madrid, Spain
Biloborodova, Tetiana	Volodymyr Dahl East Ukrainian National University, Ukraine
Caballero Morales, Santiago Omar	Universidad Popular Autónoma del Estado de Puebla, Mexico
Cano-Olivos, Patricia	Universidad Popular Autónoma del Estado de Puebla, Mexico
Casillas Martín, Sonia	Universidad de Salamanca, Spain
Cortez, Paulo	University of Minho, Portugal
Costa, Ângelo	Universidade do Minho, Portugal
Díaz-Nafría, José María	Universidad a Distancia de Madrid, Spain
Dourado, Antonio	University of Coimbra, Portugal
Duarte, Júlio	University of Minho, Portugal
Dutta, Kamlesh	National Institute of Technology, Hamirpur, India
Fajardo-Flores, Silvia	Universidad de Colima, Mexico
Fernandes, António	Instituto Politécnico de Bragança, Portugal
Fernandes, Paula Odete	Instituto Politécnico de Bragança, Portugal
Filipe Santos, Manuel	University of Minho, Portugal
Flores, Jose	Universidad Popular Autónoma del Estado de Puebla, Mexico
Gago, Pedro	Polytechnic Institute of Leiria, Portugal
Gatica, Gustavo	Universidad Andrés Bello, Chile

Gomes, Luis	Universidade dos Açores, Portugal
Gomes, Raphael	Instituto Federal de Goiás, Brazil
Guarda, Teresa	Universidad Estatal Península de Santa Elena, Ecuador
Guarnizo Marin, Jose	Universidad Santo Tomás, Colombia
Guerra, Helia	University of the Azores, Portugal
Gupta, Nishu	Vaagdevi College of Engineering, India
Härer, Felix	University of Fribourg, Switzerland
Hornink, Gabriel	Federal University of Alfenas, Brazil
Hossian, Alejandro	Universidad Tecnológica Nacional, Argentina
Ilarri, Sergio	University of Zaragoza, Spain
Khan, Fakhri	Institute of Management Sciences, Pakistan
Khattak, Asad	Zayed University, United Arab Emirates
Kirsch-Pinheiro, Manuele	Université Paris 1 Panthéon-Sorbonne, France
Lancheros-Cuesta, Diana	Universidad de la Salle, Colombia
Lenarduzzi, Valentina	LUT University, Finland
Leon, Marcelo	Universidad Tecnológica Empresarial de Guayaquil, Ecuador
Lopes, Arminda	Madeira Interactive Technologies Institute, Portugal
Lopes, Frederico	Universidade Federal do Rio Grande do Norte, Brazil
Lopes, Isabel	Instituto Politécnico de Bragança, Portugal
Machado, José	University of Minho, Portugal
Marques, Nuno	NOVA School of Science and Technology, Portugal
Martinho, Domingos	ISLA Santarém, Portugal
Martinho, Ricardo	Polytechnic Institute of Leiria, Portugal
Maskeliunas, Rytis	Kaunas University of Technology, Lithuania
Mura, Ivan	Duke Kunshan University, China
Novais, Paulo	University of Minho, Portugal
Oliveira, Pedro	Instituto Politécnico de Bragança, Portugal
Paiva, Sara	Instituto Politécnico de Viana do Castelo, Portugal
Panagiotakis, Spyros	Hellenic Mediterranean University, Greece
Peixoto, Hugo	Universidade do Minho, Portugal
Pereira, Javier	Universidad Tecnologica de Chile, Chile
Pereira, Robson	Instituto Militar, Brazil
Pérez-Montoro, Mario	Universidad de Barcelona, Spain
Pinto, Filipe	Polytechnic Institute of Leiria, Portugal
Pinto, Mario	Instituto Politécnico do Porto, Portugal
Pinto, Mónica	Universidad de Malaga, Spain
Polkowski, Zdzislaw	Jan Wyzykowski University, Poland
Pombo, Nuno	University of Beira Interior, Portugal
Portela, Filipe	Universidade do Minho, Portugal
Queirós, Ricardo	Instituto Politécnico do Porto, Portugal

Quintela, Helder	Instituto Politécnico Cávado do Ave, Portugal
Ribeiro, Maria Isabel	Instituto Politécnico Bragança, Portugal
Riboni, Daniele	University of Cagliari, Italy
Rufino, José	Polytechnic Institute of Braganca, Portugal
Rusu, Eugen	Dunarea de Jos University of Galati, Romania
Sá, Jorge	University of Minho, Portugal
Semaan, F. S.	Universidade Federal Fluminense, Brazil
Shah, Babar	Zayed University, United Arab Emirates
Sharma, Manik	DAV University, India
Simões, Alberto	Instituto Politécnico Cávado do Ave, Portugal
Sousa, Bruno	University of Coimbra, Portugal
Sousa, Maria	CIEO, Portugal
Stavrakis, Modestos	University of the Aegean, Greece
Swacha, Jakub	University of Szczecin, Poland
Tchernykh, Andrei	CICESE Research Center, Mexico
Teh, Phoey Lee	Sunway University, Malaysia
Vardasca, Ricardo	ISLA Santarém, Portugal
Verdezoto, Nervo	Cardiff University, UK
Vicente, Henrique	Universidade de Évora, Portugal
Vieira de Castro, António	Instituto Politécnico do Porto, Portugal
Wei, Ran	Dalian University of Technology, China
Zolotas, Athanasios	University of York, UK

Sponsors

Universidad Estatal Peninsula de Santa Elena, Ecuador

Universidade do Minho, Portugal

ISLA Santarem, Portugal

Universidad Tecnológica Empresarial de Guayaquil, Ecuador

Institute of Management Sciences, Pakistan

BITrum Interdisciplinary Research Group

UNIAG, Portugal

Universidad a Distancia de Madrid, Spain

Instituto de Investigación Científica y Desarrollo Tecnológico

Ethics, Security, and Privacy

Computational Modeling of the Thermal Effects on Composite Slabs Under Fire Conditions

Carlos Balsa[1(✉)], Matheus B. Silveira[2], Valerian Mange[3], and Paulo A. G. Piloto[4]

[1] Research Centre in Digitalization and Intelligent Robotics (CeDRI), Instituto Politécnico de Bragança, Bragança, Portugal
balsa@ipb.pt
[2] Universidade Tecnológica Federal do Paraná, Campus Pato Branco, Via do Conhecimento, s/n - KM 01 - Fraron, Pato Branco, PR 85503-390, Brazil
matheussilveira@alunos.utfpr.edu.br
[3] ENSEEIHT - IRIT-UFTMiP, Toulouse, France
valerian.mange@etu.toulouse-inp.fr
[4] LAETA-INEGI and Instituto Politécnico de Bragança, Bragança, Portugal
ppiloto@ipb.pt

Abstract. This paper presents finite element thermal models to evaluate the thermal behavior of composite slabs with steel deck, submitted to standard fire exposure. Composite steel/concrete slabs are a mix of a reinforced concrete layer with a profiled steel deck reinforced by steel bars between its ribs. The resulting transient and non-linear thermal problems are solved numerically with three-dimensional multi-domain finite element models. The models were developed for normal weight concrete and lightweight concrete, and for different steel deck geometries (trapezoidal and re-entrant). The results of the numerical simulations are used to present a new calculation method to determinate the temperatures on the steel deck components and on the rebars and, consequently, to determine the bending resistance of composite slabs under fire conditions.

Keywords: Nonlinear energy equation · Finite element method · Composite slab · Standard fire · Fire rating

1 Introduction

Composite steel/concrete slabs are an alternative construction elements that ensure some advantages to structures, such as the reduction of the self-weight of the structures while speeding up the construction process. The slabs are composed by a profiled steel deck which can be used as permanent formwork, and a reinforced concrete placed on the top (see Fig. 1). The use of composite slabs in buildings has become very popular in North America since 1960. However, due to the fact that there was insufficient information regarding its structural safety, only after 1980 has become popular in Europe. The slab's overall depth usually varies between 100 to 170 mm. The thickness and geometry of the steel deck depends on the producer of the profiles, and usually includes a zinc coating on the exposed surface to resist corrosion [8].

T. Guarda et al. (Eds.): ARTIIS 2021, CCIS 1485, pp. 497–511, 2021.
https://doi.org/10.1007/978-3-030-90241-4_38

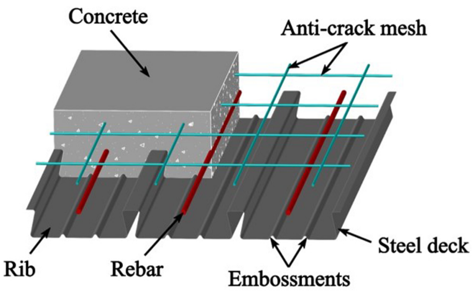

Fig. 1. Composite slab with trapezoidal steel deck (adapted from [14]).

In addition to the corrosion problem, the composite slabs may suffer significant damage when exposed to fire, since the steel elements which are responsible for ensuring the slabs bending resistance capacity are significantly affected under fire conditions. Therefore, it is necessary to perform a thermal analysis previously to the structural analysis, thus guaranteeing that this building element has the fire resistance according to regulations and standards. The fire rating of this type of element is then determined by standard fire tests, accounting for load-bearing (R), Integrity (E), and Thermal Insulation (I). This means that for a composite slab to demonstrate the fire resistance in agreement to the criteria established by the European standard EN 13501-2 [5], it must have the capacity to prevent large deformation or rate of deformation whenever in service, which means the load-bearing, it must also provide thermal insulation, thus limiting the increase in temperature on the unexposed side. Finally, the slabs must keep fire in the exposed side, preventing the passage of flames and hot gases through cracks or holes, which comprises the Integrity criterion.

This work is concerned with the determination of the thermal behavior of composite slabs under a standard ISO-834 fire [9], specially focused on the temperature evolution on the components of steel deck (upper flange, web, lower flange), and the rebars. An accurate and reliable estimation of the temperatures in these components is required, especially to determine the load-bearing criterion, since these temperatures directly influence the steel and concrete strength reduction factors and consequently the bending resistance of the slabs.

Among several ways to determine the fire rating of a composite slab, the development of experimental standard fire tests are the most expensive and time-consuming. Alternatively, the Annex D of the EN 1994-1-2 [4] provides the guidelines for estimating the fire resistance based on the simplified calculation method, but this method is based on studies that have been carried out a long time ago and are currently outdated. The third method consists of simulating the experimental fire tests through finite elements. Computational simulations are of great importance in this field because this can promote a reliable and realistic description of the physical phenomena.

The year of 1983 was very important to the dissemination of composite slabs as an alternative and functional construction process. In this year, the European Convention for Constructional Steelwork ECCS [7], published the design rules for composite concrete slabs with a profiled steel deck, exposed to a standard fire. According to this document, the explicit fire design calculation for composite slabs is not required when the fire requirements are smaller or equal than 30 min and for other fire rating the calculation methods were based on conservative approximations for a safer design procedure. This standard was developed to guarantee structural safety according to the fire resistance classes established by ISO 834-1 [9] without the obligation to carry out experimental tests. This document should only be applied if the composite slab was safely designed for room temperature.

Hamerlinck was a pioneer in proposing mathematical models to estimate the fire resistance of composite slabs. In 1990, he proposed a numerical calculation model that includes thermal and mechanical models for the cross-section analysis and a structural analysis model for composite slabs [8]. Later, in 1991, Hamerlinck [8] describes in detail all the methods conducting numerical and experimental studies regarding the thermal and mechanical behaviour of reinforced composite slabs under fire. Current standards are still based on his work.

In the last years, an extensive range of thermal and structural models have been developed in different finite element software to predict the structural behavior of steel-concrete composite slabs under fire conditions. In 2018, Piloto et al. [18] analyzed the fire resistance of composite concrete slabs with profiled steel deck, in this case also reinforced by a steel mesh at the topside, including reinforcing bars between its ribs. The key objective of this study was to develop two-dimensional numerical models using the Matlab and ANSYS softwares in order to evaluate the fire resistance of different slab configurations according to the insulation criterion. For the development of this research, the fire rating for insulation (I) criterion was evaluated using numerical and simple calculation methods, and then validated against experimental fire tests. The results obtained by the authors allowed the demonstration of the fire resistance (I) increase with concrete thickness for both calculation methods. However, using the numerical method, the simulation predicts a lower fire resistance (I) when compared to fundamental standards, consequently ensuring more structural safety when using this method. Therefore, a new and better approach was proposed, considering a quadratic variation between the fire resistance and the effective thickness of the composite slab. More recently, the same methodology was applied to different slab geometries under the action of different types of standard fires in [14–17].

In 2021 Bolina et al. [1], determined the thermal behavior of composite steel-concrete slabs exposed to a standard fire. The main objective of the work was to develop a comparison of the temperature distribution in the cross-section through several methods: experimental, numerical, and analytical. The authors carried out eight full-scale fire tests which were used to calibrate the numerical models developed using the ABAQUS software. The numerical methods were compared with the analytical method provided by Eurocode 1994-1.2 [4]. The authors noticed a convergence of the analytical method with the numerical and experimental methods only for the steel deck, but not for the concrete, the rebars (positive and negative), and the thermal insulation. Therefore, a new analytical approach was developed to determine the temperature in the rebars and new factors to evaluate the performance of the thermal insulation.

In the present work, aiming to optimize the analytical temperature calculation presented by the simplified calculation method provided in the Annex D of Eurocode

1994 1-2, a parametric study was performed in order to analyze the thermal behavior of composite slabs. The temperature distribution along slabs using normal weight and lightweight concrete (NWC and LWC) was determined for four different types of steel deck geometries, which were chosen to present two different geometric classes, trapezoidal and re-entrant, using different concrete thickness over the steel deck h_1.

Three-dimensional models are presented to simulate the thermal effects of standard fire exposure on composite slabs. The reduce scale models where simulated with three dimensional finite elements using the Matlab Partial Differential Equations Toolbox (PDE Toolbox) [12]. The numerical models comprise different physical domains with different thermal properties, corresponding to the components of the slab such as concrete, steel deck and rebars. In addition, to simulate the debonding effects, air-gap with 0.5 mm of constant thickness is included between the steel deck and concrete.

The heat transfer problem is solved numerically through the Finite Element Method (FEM) with thermal models, already validated with experimental tests by Piloto et al. [13, 18], available in the Matlab PDE Toolbox. The temperature evolution on the steel deck components and on the rebars is evaluated for all the four different composite slabs with different concrete thickness h_1, and subsequently the results are compared with the simplified method provided in the Annex D of Eurocode 1994-1.2. Additionally, a new formula based on the parametric results is proposed to analytically calculate the temperature of slabs components.

2 Heat Transfer Problem

This section presents all the methodology necessary to develop the finite element thermal model, which will be used to solve the nonlinear transient thermal problems. Therefore, the heat transfer problem in this study has to be solved in the multi-domain body corresponding to the composite slab under standard fire conditions. It is worth mentioning that the heat flux applied to the unexposed side depends on the ambient temperature and the heat flux applied to the exposed side depends on the standard fire established by the ISO-834 fire curve.

2.1 Physical Domains

The three-dimensional (3D) transient heat transfer problems will be solved on four different composite slabs with different geometries presented in Fig. 2. First, two composite slabs with trapezoidal geometry were selected: Confraplus 60 and Polydeck 59 s. For this category, the following values were adopted for the h_1 thickness: 50, 70, 90, 110, and 125 mm. However, for other two slabs with re-entrant geometry (Multideck 50 and Bondek) the following thicknesses h_1 where used: 60, 70, 90, 110, and 125 mm.

The 3D models were developed in agreement with a realistic representation of the composite slabs physical model. The geometry of the models consider the exact shape of the surfaces from a representative volume of the slab. The cross-section which was selected has the side edges delimited by the centroid of the upper flange and comprising one rib. The length of the specimens is 250 mm (see Fig. 3).

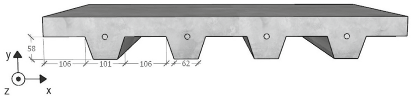

(a) Confraplus 60 geometric characteristics.

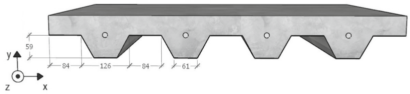

(b) Polydeck 59S geometric characteristics.

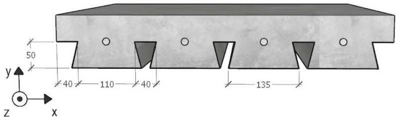

(c) Multideck 50 geometric characteristics.

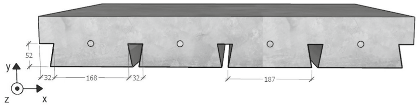

(d) Bondek geometric characteristics.

Fig. 2. Composite slabs geometric characteristics and dimensions [mm].

The multi-domain developed comprises four sub-domains: the steel deck, the airgap, the concrete, and the rebar. Thus, the materials that compose the physical subdomains of the slabs are carbon steel (steel deck and rebars), the concrete (concrete topping), and airgap (to simulate the debonding effect between the steel deck and concrete).

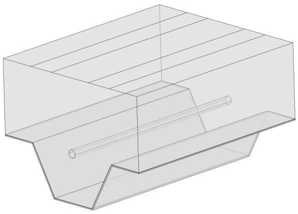

(a) Slab Geometry.

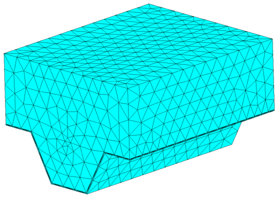

(b) Finite Element Mesh.

Fig. 3. Example of a modelled composite slabs specimen [mm].

Confraplus 60 is a trapezoidal model profile produced by ArcelorMittal. The colaborating steel deck is produced with S350 steel and the model with 1.25 mm of thickness has been selected. The geometric characteristics are presented in the Fig. 2(a). The Polydeck 59S model is the second trapezoidal profile selected. The Polydeck 59S model from ArcelorMittal, presented in Fig. 2(b) is made by a steel deck with S450 steel and 1 mm of thickness. The re-entrant model presented in Fig. 2(c) is the Multideck 50 produced by Kingspan Structural Products. This product has a steel profile with steel grade S450 and 1 mm of thickness. The second type of re-entrant slab studied is Bondek, which is developed and produced by the Lysaght company. The deck consists of a steel profile with grade S350 and the 1 mm thickness model was selected (see Fig. 2(d)). These geometries have been selected based on the geometric difference and current use.

The heat transfer inside the models, through the discretization of the domain in a finite element mesh as illustrated in Fig. 3, is exclusively made by conduction. The heat conduction inside the physical domain is mathematically modelled by the energy conservation equation

$$\rho\left(T\right)C_p\left(T\right)\frac{\partial T}{\partial t} = \nabla\cdot\left(\lambda\left(T\right)\nabla T\right), \tag{1}$$

where T represents the temperature (°C), $\rho(T)$ is the specific mass (kg/m^3), $Cp(T)$ is the specific heat (J/kgK), $\lambda(T)$ is the thermal conductivity (W/mK), t is the time (s) and $\nabla = (\partial_x, \partial_y, \partial_z)$ is the gradient. Equation (1), is based on the heat flow balance, for the infinitesimal material volume, in each spatial direction.

The thermal properties of the materials that compose the slabs are determined by the Eurocodes [2–4] (steel and concretes) and by [6] (air), and are temperature dependent. Therefore, the specific mass $\rho(T)$, the specific heat $Cp(T)$ and the thermal conductivity $\lambda(T)$ vary with the temperature, introducing the non-linearity of the Eq. (1). Figure 4 describes the thermal properties of the four different types of materials that constitute the studied composite slabs.

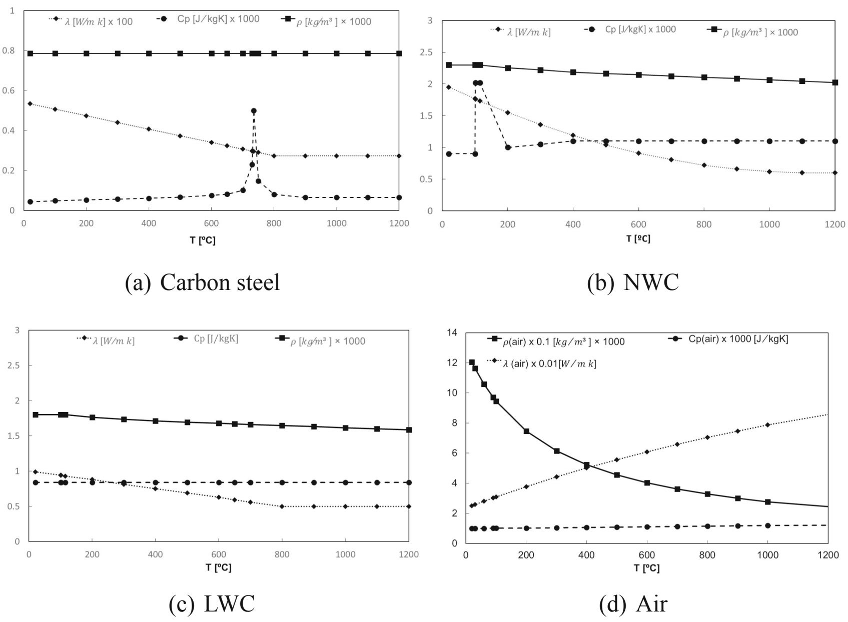

(a) Carbon steel (b) NWC

(c) LWC (d) Air

Fig. 4. Thermal properties of composite slab components.

Once the heat flux on the fire exposed surface changes with time, the Eq. (1) is time-dependent and holds a transient thermal state for the slab. So, in order to determine the temperature field along the time, the solution of Eq. 1 is required. Furthermore, for the correct solution of the problem, it is necessary to apply the boundary conditions according to the ISO-834 fire curve in the physical domain.

2.2 Boundary Conditions

The boundary conditions are used in numerical simulations to solve the differential equations intrinsic to the model. Therefore it is necessary to master the different natures of heat transfer that act on the slabs, that is, the conduction, convection, and radiation. In thermal analysis, the finite element mesh is generally used to model solids in which conduction is the predominant heat transfer method, and the radiation and convection are imposed through boundary conditions. The composite slabs are subjected to three main boundary conditions comprising the exposed surface, the unexposed surface, and the adiabatic surfaces. All of them follow the guidelines of Eurocode 1991-1.2 [4].

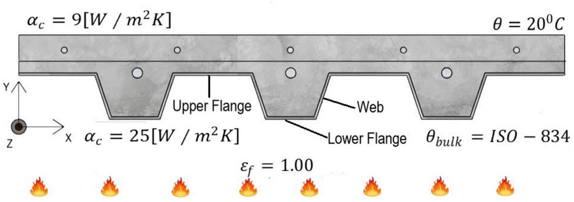

Fig. 5. Boundary conditions.

The boundary conditions in the exposed side of the slab, comprise the heat transfer by convection and radiation and are given by

$$\lambda(T)\nabla T.\vec{n} = \alpha_c(T_\infty - T) + \phi\varepsilon_m\varepsilon_f\sigma\left(T_\infty^4 - T^4\right) \tag{2}$$

where $\vec{n}$ is the unitary vector normal to the external face, ϕ is the view factor, α_c is the convection coefficient, ε_m is the emissivity of the material, ε_f is the emissivity of fire, σ is the Stefan-Boltzmann constant and T_∞ is the gas temperature of the fire compartment. In Eq. (2), the convection coefficient is $\alpha_c = 25$ W/m^{2}K, the emissivity of steel is $\varepsilon_m = 0.7$ and the fire emissivity is $\varepsilon_f = 1$. This equation represents the amount of energy (or the heat flow) that arrives to the steel deck by radiation and convection based on the gas bulk temperature, which will be transferred though the slab by conduction. The boundary conditions parameters are represented in Fig. 5.

The view factor (ϕ) is a term of great relevance in studying the thermal behavior of structures exposed to fire, that quantifies the geometric relation between the surface emitting radiation and the receiving surface. Thus, it is an adimensional parameter and dependends on the rib surfaces orientations, and the distance between the radiative surfaces. The emissivity for the lower flange is 1 and the values for the web and upper flange are usually smaller than 1.

The view factor has high variability due to complexity in its determination. For this reason, to determine the view factor associated with web and upper flange of steel deck, the Crossed-Strings Method, proposed by Hotell H. C. in 1950 [6], was used in this study. Following this rule, Fig. 6 shows the parameters required for the approximation of the view factor in composite slabs.

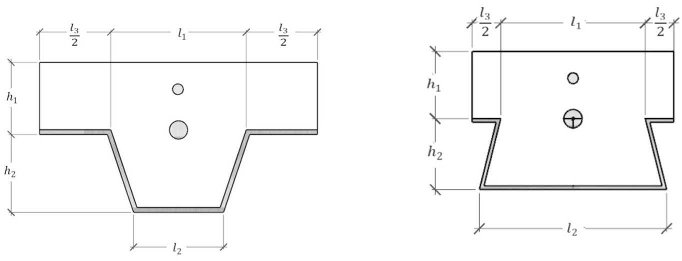

(a) Trapezoidal (b) Re-entrant

Fig. 6. Geometric parameters used to determine view factors according to each slab profile.

The view factor of the lower flange is $\phi = 1$, and the resulting equations for the upper flange (ϕ_{up}) and web (ϕ_{web}) view factors are presented in Eqs. (3) and (4).

$$\phi_{up} = \frac{\sqrt{h_2^2 + \left(l_3 + \frac{l_1 - l_2}{2}\right)^2} - \sqrt{h_2^2 + \left(\frac{l_1 - l_2}{2}\right)^2}}{l_3} \tag{3}$$

$$\phi_{web} = \frac{\sqrt{h_2^2 + \left(\frac{l_1 - l_2}{2}\right)^2} + (l_3 + l_1 - l_2) - \sqrt{h_2^2 + \left(l_3 + \frac{l_1 - l_2}{2}\right)^2}}{2\sqrt{h_2^2 + \left(\frac{l_1 - l_2}{2}\right)^2}} \tag{4}$$

The Eq. (5) presents the gas temperature of the fire compartment following the standard fire curve ISO-834 ($T_\infty = T_{ISO}$) given by

$$T_{ISO} = 20 + 345 \log_{10}(8t + 1), \tag{5}$$

where T_{ISO} is given in °C and t in minutes [9].

The top part of the composite slab (unexposed side) is also an important side to determine the temperature evolution. After all, it will determine the heat transfer from the slab to the above compartment allowing the calculation of the fire resistance with respect to the insulation criterion. Following the Eurocode recommendations, the heat effect on the unexposed side may be defined by the heat flux by convection, using $\alpha_c = 9$ W/m^{2}K, to include the radiation effect [3]. The boundary condition in the upper surface of the slab is given by Eq. (6),

$$\lambda(T)\nabla T.\vec{n} = \alpha_c (T - T_\infty) \tag{6}$$

where T_∞ is the room temperature.

The other four surfaces of the slab (front, back, left and right) are considered insulated, i.e., the boundary conditions applied to these faces are given by Eq. (7),

$$\lambda(T)\nabla T.\vec{n} = 0 \tag{7}$$

Equation (7) which is based on the adiabatic condition, applied to the external lateral surfaces of the slab.

3 Numerical Solution Through Finite Element Method

In order to perform a thermal analysis on composite slabs, the Eq. (1) must be solved through the FEM on 3D domain using Matlab PDE Toolbox. The generated thermal models are composed of sub-domains corresponding to different materials with 3D finite elements resulting from the discretization of the domain (see Fig. 3).

Equation (1) is solved by FEM based on the weak-form Galerkin model and the minimum condition to the weighted residual method, thus leading to the energy matrix formulae

$$C(T)\dot{T}+K(T)T=F \tag{8}$$

where C is the capacitance matrix, $\dot{T}$ is the vector of time derivatives of the temperatures, K is the conductivity matrix and F is the vector of the thermal loads (for details see, for instance, [10]). The vector of the thermal loads F includes the boundary conditions. The solution of the first order non-linear system of ordinary differential equations given by Eq. (8), considering $T(t_0)=T^0$ and the boundary conditions, enables to determine the temperature at each node of the finite element mesh, illustrated in Fig. 3 (b), over the time interval $\left[t_0,\ t_f\right]$.

3.1 Computational Solution with Matlab

The Matlab (R2019a) PDE Toolbox was used to develop and solve the nonlinear transient thermal analysis. The finite element model of the composite slab created with Matlab uses only one type of finite element. The tetrahedral finite elements are defined by four nodes and use linear interpolation functions. The finite element mesh is composed by four different sub-domains: concrete, steel deck, rebar and air-gap. Thus, 3 different materials are used (concrete, steel and air). Additionally, two different types of concrete are considered: NWC and LWC.

Regarding the finite element mesh size on the models, the maximum mesh edge length varies according to each steel deck profile. Figure 3 (b) presents the finite element mesh in one of the studied models, in which the element size was selected by a convergence of results with the mesh refinement, which means the size of mesh elements was adjusted until the relative error in nodal temperature calculations has the maximum value of 10^{-4} in the worst scenario.

In Matlab PDE Toolbox the Eq. (8) is converted in

$$C(T)\dot{T}=\bar{F}\left(T\right) \tag{9}$$

where $\bar{F}\left(T\right)=F-K(T)$. The solution of Eq. (9) is computed by the built-in function `ode15s` [19]. The algorithm implemented in this function is based on the discretization of the time derivative by numerical differentiation formulas (NDFs) of orders 1 to 5. The order of accuracy of the solution can be explicitly controlled through the absolute or relative tolerance parameters. In this work a value of 10^{-6} is set to the absolute tolerance, and 10^{-3} is set to the relative tolerance. In each time step, the non-linear system of algebraic equation is solved through the Newton-Raphson method whose stopping criterion can be monitored by means of the maximal number of iterations, set to 25, and the residual tolerance, set to 10^{-4} (for more details see [12]).

4 Simplified Calculation Method and Numerical Results

A parametric study is conducted in order to investigate the influence of the concrete thickness h_1 on the temperatures used to determine the fire resistance of composite slabs according to the load-bearing criterion (R). As already mentioned, the load-bearing resistance depends on the temperatures in the steel deck components and rebar. A simplified calculation method is proposed by the standard Eurocode 1994 1.2 [4]. But this model hasn't been updated for a long time and needs to be revised. The proposed methodology is based on solving numerically the thermal problem, presented in the previous section, for different thicknesses of the concrete cover (h_1) and compare the results with the simplified method.

4.1 Simplified Calculation Method

The simplified calculation method used for the load-bearing criterion (R) presented in Eurocode 1994 1.2 [4] can be applied to simply support composite slabs when exposed to an ISO-834 standard fire [9]. In order to calculate the bending moment resistance of the composite slab (sagging moment), the standard defines the temperature for each steel deck component (upper flange, web and, lower flange) according to the formula

$$\theta_a = b_0 + b_1 \frac{1}{l_3} + b_2 \frac{A}{L_r} + b_3 \phi + b_4 \phi^2 \tag{10}$$

and the rebar component θ_s by the formula

$$\theta_s = c_0 + c_1 \frac{u_3}{h_2} + c_2 z + c_3 \frac{A}{L_r} + c_4 \alpha + c_5 \frac{1}{l_3} \tag{11}$$

where the temperatures θ_a and θ_s are given in [$^\circ C$], the parameter ϕ is adimensional and corresponds to the view factor of the steel deck component (upper flange only), given by Eq. 3, and the terms b_i and c_i refer to the coefficients given by Eurocode 1994 1.2 [4], which depends on the type of concrete used in the composite element and changes according to the standard fire resistance that must be achieved. The component u_3 represents the distance from the rib centroid to the lower flange in [mm], the z-factor represents the position of the rebar concerning the slab rib given in [mm$^{-0.5}$], and the term α corresponds to the angle formed between the web component of the steel deck and the horizontal direction in degrees [$^\circ$].

4.2 Numerical Results

A total of 40 numerical simulations were carried out, using an air-gap of 0.5 mm. This air-gap value has been obtained through the previous calibration [13]. The computational simulations took into account h_1 values equal to 60, 70, 90, 110, and 125 mm for the two trapezoidal geometries (see Figs. 2 (a) and (b)), and equal to 50, 70, 90, 110, and 125 mm for the two re-entrant geometries (see Figs. 2 (c) and (d)). All simulations were done for NWC and LWC.

Figure 7 and Fig. 8 show the distribution of temperatures inside the slab after 120 min and the evolution of average temperatures, computed numerically (N), in the three parts of the steel deck and in the rebar. For comparison, values calculated using the simplified method (S), given by Eqs. 10 and 11 are also included. Additionally, the T_{ISO} given by Eq. 5 is also depicted in these figures.

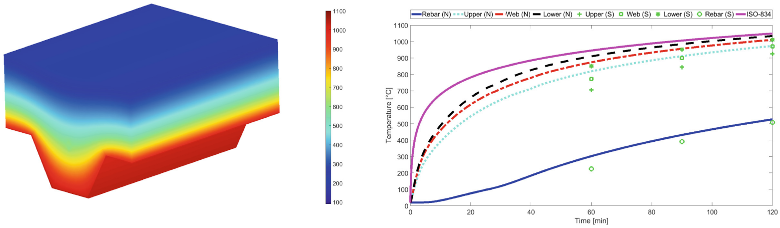

(a) Final temperature distribution (b) Temperature evolution

Fig. 7. Polydeck 59S with NWC.

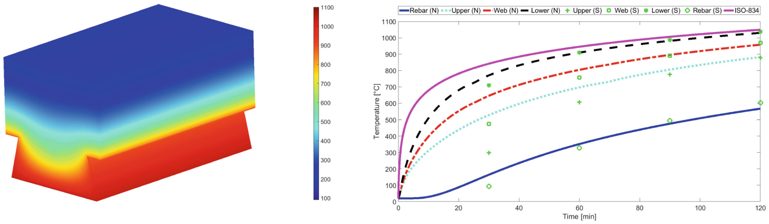

(a) Final temperature distribution (b) Temperature evolution

Fig. 8. Multideck 50 with LWC.

Figure 7 shows the thermal behavior of the trapezoidal Polydeck 59S slab with $h_1 =$ 90 mm using NWC, and Fig. 8 presents the thermal behavior of the re-entrant Multideck 50 slab with $h_1 = 90$ mm using LWC. It is observable that, in general, the temperatures predicted by the simplified model are below the numerical results. This is especially true for the fire ratings of 30 and 60 min, in the case of the Multideck 50, and 60 min, in the case of the Polideck 59S geometry.

4.3 New Calculation Proposal

Based on the simulation results, new coefficients b_i and c_i are proposed for the simplified model. In addition, the original models, given by Eqs. 10 and 11, are modified by including a new term that depends on h_1, in order to take into account the effect on temperatures of the thickness of the concrete topping. The thickness h_1 is explicitly included in the model multiplied by coefficient b_5, in the case of the steel deck temperatures, and by c_6, in the case of the rebar temperature. Thus, the new proposal for the steel deck temperature is

$$\theta_a = b_0 + b_1 \frac{1}{l_3} + b_2 \frac{A}{L_r} + b_3 \phi + b_4 \phi^2 + b_5 h_1 \tag{12}$$

and for the rebar is

$$\theta_s = c_0 + c_1 \frac{u_3}{h_2} + c_2 z + c_3 \frac{A}{L_r} + c_4 \alpha + c_5 \frac{1}{l_3} + c_6 h_1. \tag{13}$$

The coefficients for these new proposal methods have been determined by fitting the mathematical models, represented by Eqs. 12 and 13, to the numerical results obtained with the parametric study with h_1, two different types of concrete and the four different composite slab geometries. The coefficients were determined using the nonlinear least-squares method. This method consists of minimizing the sum of the squared deviations between the temperatures proposed by Eqs. 12 or 13 and those obtained through simulations. This sum was minimized using the Generalized Reduced Gradient (GRG) nonlinear solver [11].

The resulting coefficients for the calculation of temperatures on the steel deck components, through Eqs. 12, are presented in Table 1. For the calculation of the temperatures on the rebar, through Eqs. 13, the proposed coefficients are presented in Table 2. It is worth mentioning that additionally to the standard fire resistance ratings of 60, 90 and 120 min for NWC and 30, 60, 90 and 120 min for LWC, the new proposal also comprises the coefficients for the fire rating of 45 min.

4.4 Comparing Results

In order to verify the differences between the Eurocode 1994-1.2 [4] for the simplified method (S), the numeric results (N), and the new calculation proposal (P), comparison graphs were developed. Figure 9 a) establish this comparison for each steel deck component and the rebars for NWC, while Fig. 9 b) plays the same role for LWC.

Comparing with the Eurocode proposal, the new proposal contributes to improve the temperature estimation according to each fire resistance time. For both types of concrete (NWC and LWC), the new proposal matches very well with the numerical results. It is also possible to verify that the analytical method, proposed by the Eurocode, predicted much lower temperatures than the numerical results, mainly for lowest fire ratings.

Table 1. New b_i coefficients proposal for the steel deck components.

Concrete	Fire resist.	Flange	b_0	b_1	b_2	b_3	b_4	b_5
NWC	45 min	Upper	139.9655	620.7460	7.6958	1421.9882	−1204.0686	−0.0564
		Web	404.1556	−1623.2839	6.7521	1109.9125	−1060.6480	−0.0187
		Lower	860.8523	−2427.8085	1.0349	−40.2277	36.9805	−0.0033
	60 min	Upper	224.5881	−2852.6026	10.8539	1428.8794	−1312.5261	−0.1046
		Web	599.8829	−13427.3660	17.2020	327.3531	−522.0016	−0.0346
		Lower	917.5108	−3173.1570	2.0515	−47.7229	15.2644	−0.0061
	90 min	Upper	578.7070	−18369.1630	22.9583	139.6578	−322.2799	−0.1799
		Web	542.0284	633.9895	4.6194	1398.3091	−1361.2018	−0.0674
		Lower	982.2585	−3077.4610	2.3687	3.3250	−52.4300	−0.0166
	120 min	Upper	691.0625	−14595.5356	18.2749	212.0806	−340.0106	−0.2667
		Web	666.1045	−416.2267	4.8378	1158.5088	−1146.7154	−0.1088
		Lower	955.4042	4109.1835	−3.8674	492.9857	−407.7782	−0.0189
LWC	30 min	Upper	302.1644	−5233.6445	10.9946	614.9448	−529.2700	−0.0111
		Web	491.6762	−3193.5831	6.6500	522.4295	−491.2013	−0.0003
		Lower	871.2783	−4956.7858	3.0851	−469.3452	438.6676	0.0006
	45 min	Upper	388.5675	−7171.2080	12.8469	755.4877	−743.7176	−0.0422
		Web	486.1987	1073.6509	3.5221	1137.2531	−1073.2821	−0.0110
		Lower	868.1465	−1328.8180	0.6831	22.4003	−24.4881	−0.0005
	60 min	Upper	389.9821	114.9104	5.8948	1325.8176	−1200.0499	−0.0713
		Web	632.6120	−4880.4634	8.4873	662.5945	−722.1706	−0.0232
		Lower	904.4639	−277.6849	−0.0679	115.2137	−106.1585	−0.0026
	90 min	Upper	578.3817	−425.0477	4.8700	1042.2053	−944.7059	−0.1217
		Web	629.7576	5806.3988	−1.5116	1364.7899	−1243.5193	−0.0478
		Lower	986.6232	−834.2380	0.4527	39.8315	−44.2602	−0.0070
	120 min	Upper	686.5569	1931.2433	1.5912	994.6118	−861.4596	−0.1382
		Web	820.5056	−1457.3952	4.0784	632.9442	−642.8140	−0.0599
		Lower	1042.9854	−1215.3431	0.8033	−14.9962	2.3697	−0.0108

Table 2. New c_i coefficients proposal for the rebars.

Concrete	Fire resist.	c_0	c_1	c_2	c_3	c_4	c_5	c_6
NWC	45 min	99.8233	100.1983	106.0042	−11.8333	2.0660	−3983.0834	−0.0566
	60 min	−880.0008	923.7717	389.1767	−30.6981	2.9630	−5263.7252	−0.1241
	90 min	117.6928	961.6281	−526.6992	28.0940	0.7423	−5803.2055	−0.3510
	120 min	−151.2236	834.6475	31.9477	−8.0649	2.2052	−7000.3192	−0.6032
LWC	30 min	−496.7732	430.0693	326.4075	−25.8183	2.4637	−3419.6974	−0.0099
	45 min	−2463.4757	2829.0060	49.4180	−9.8686	2.0244	−4509.8827	−0.0558
	60 min	317.3687	53.5299	179.5837	−19.0716	2.4341	−5491.2669	−0.1346
	90 min	528.3687	−181.2998	395.2534	−33.4968	2.9036	−6393.0551	−0.3148
	120 min	−373.7261	−325.9842	1616.5151	−112.2265	6.0518	−7756.3731	−0.4362

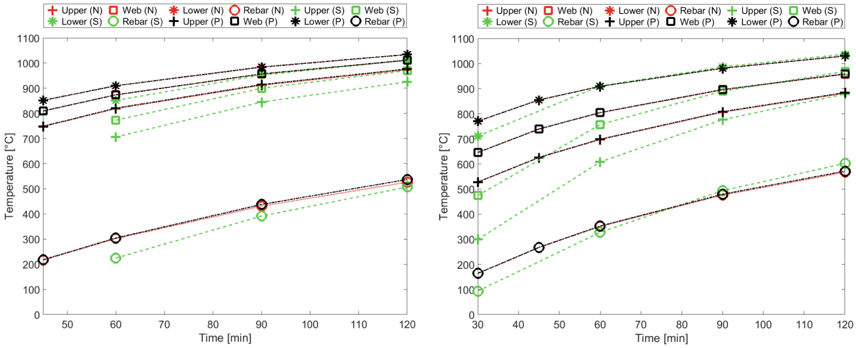

(a) Polydeck 59S with NWC (b) Multideck 50 with LWC

Fig. 9. Temperature corresponding to different fire rating times.

5 Final Considerations

In this work, new and more realistic computational models were developed to represent the thermal behavior of composite slabs under standard fire conditions. The results of the parametric analysis enable us to determine the temperatures for different slab geometries and compare them with the ones provided by the simplified calculation method of Eurocode 1994-1.2. The new proposed model aimed to comprise some effects that the current Eurocode neglects, such as the debonding effect between the steel deck and concrete and the thickness of the concrete topping.

In order to optimize the analytical calculation proposal, a new calculation proposal for determining the temperature in the steel deck components and the rebars based on the numerical results is presented. The new formulation includes in the actual formula, provided by the Eurocode, an additional term in order to include the effect of the concrete thickness. The new coefficients were determined by fitting the new proposal to the numerical results by non-linear least-squares. The new proposal provide an improvement of the temperature estimation that affects the reduction coefficients in all the slab components and, consequently, an accurate estimation of the load-bearing resistance criteria. The load-bearing resistance criteria will be based on the reduction coefficients applied to yield strength of each component. Future work should include the moisture effect in the thermal behaviour of the concrete and the mechanical effect of the airgap on the load-bearing capacity.

Acknowledgements. This work has been supported by FCT - Fundação para a Ciência e Tecnologia within the Project Scope: UIDB/05757/2020.

References

1. Bolina, F., Tutikian, B., Rodrigues, J.P.C.: Thermal analysis of steel decking concrete slabs in case of fire. Fire Saf. J. **121**, 103295 (2021). https://doi.org/10.1016/j.firesaf.2021.103295

2. CEN: EN 1993-1-2: Design of steel structures. Part 1–2: General rules - structural fire design eurocode (2002)
3. CEN: EN 1992-1-2: Design of concrete structures. Part 1–2: General rules - structural fire design (2004)
4. CEN: EN 1994-1-2: Design of composite steel and concrete structures. Part 1–2: General rules - structural fire design (2005)
5. CEN: EN 13501-2: Fire classification of construction products and building elements. (2016)
6. Cengel, Y.A., Ghajar, A.J.: Heat and Mass Transfer: Fundamentals and Applications. McGraw-Hill Education, Europe (2014)
7. ECCS: Calculation of the fire resistance of composite concrete slabs with profiled steel sheet exposed to the standard fire (1983)
8. Hamerlinck, A.F.: The behaviour of fire-exposed composite steel/concrete slabs. Ph.D. thesis, Eindhoven University of Technology (1991)
9. ISO: International standard ISO 834 - fire-resistance tests: Elements of building construction (1975)
10. Gartling, D.K., Reddy, J.N.: The Finite Element Method in Heat Transfer and Fluid Dynamics, 3 edn. CRC Press, Boca Raton (2010)
11. Lasdon, L.S., Fox, R.L., Ratner, M.W.: Nonlinear optimization using the generalized reduced gradient method. Revue française d'automatique, informatique, recherche opérationnelle. Recherche opérationnelle **8**(V3), 73–103 (1974). https://doi.org/10.1051/ro/197408v300731
12. MathWorks: Partial Differential Equation Toolbox™ User's Guide, Heat Transfer Problem with Temperature-Dependent Properties. The MathWorks, Inc.
13. Piloto, P.A.G., Balsa, C., Ribeiro, F.F., Santos, L.M., Rigobello, R., Kimura, É.: Three-dimensional numerical modelling of fire exposed composite slabs with steel deck. MATTER Int. J. Sci. Technol. **5**(2), 48–67 (2019). https://doi.org/10.20319/mijst.2019.52.4867
14. Piloto, P.A.G., Balsa, C., Ribeiro, F.F., Rigobello, R.: A new calculation method for the temperature of the components of composite slabs under fire. J. Comput. Appl. Mech. (2021). https://doi.org/10.22059/jcamech.2021.316216.584
15. Piloto, P.A.G., Balsa, C., Ribeiro, F.F., Rigobello, R.: Three-dimensional numerical analysis on the fire behaviour of composite slabs with steel deck. In: Piloto, P.A.G., Rodrigues, J.P., Silva, V.P. (eds.) CILASCI 2019. LNCE, vol. 1, pp. 12–30. Springer, Cham (2020). https://doi.org/10.1007/978-3-030-36240-9_2
16. Piloto, P.A.G., Balsa, C., Ribeiro, F., Rigobello, R.: Computational simulation of the thermal effects on composite slabs under fire conditions. Math. Comput. Sci. **15**(1), 155–171 (2020). https://doi.org/10.1007/s11786-020-00466-0
17. Piloto, P.A.G., Balsa, C., Santos, L.M., Kimura, É.F.: Effect of the load level on the resistance of composite slabs with steel decking under fire conditions. J. Fire Sci. **38**(2), 212–231 (2020). https://doi.org/10.1177/0734904119892210
18. Piloto, P.A.G., Prates, L., Balsa, C., Rigobello, R.: Numerical simulation of the fire resistance of composite slabs with steel deck. Int. J. Eng. Technol. **7**(2.23), 83 (2018). https://doi.org/10.14419/ijet.v7i2.23.11889
19. Shampine, L.F., Reichelt, M.W.: The MATLAB ODE suite. SIAM J. Sci. Comput. **18**(1), 1–22 (1997)